

# Chapter 2

## Optical Propagation in Unguided Media

Yahya Kemal Baykal

**Abstract** This chapter provides fundamentals of light propagation in unguided media and particularly discusses turbulence of transmission environment. The degradation effects of turbulence in the received signal of an OWC system are presented. The turbulence power spectra used in the formulation of various entities are given in various links operating in different environments such as atmosphere, space and underwater. The Rytov method and the extended Huygens–Fresnel principle are employed in the evaluation of the average intensity and the scintillation index. Effects of different optical beam profiles in the average received intensity and the scintillation index are further examined. Finally, some mitigation methods, such as the transmitter and the receiver aperture averaging, to reduce the turbulence degradation are given.

**Keywords** Atmospheric turbulence • Underwater turbulence • Free space optics • Optical wave propagation • Unguided media • Optical beam types • Average intensity • Scintillations

### 2.1 Introduction

Optical wave propagating in an unguided medium such as the atmosphere or underwater has to go through many constituents such as the molecules and aerosols in the case of propagation in the atmosphere and water molecules, chlorophyll, coloured dissolved organic matters, suspended particulate matters and dissolved salts in the case of propagation in underwater medium with different concentrations in freshwater or marine environment. These constituents cause the optical wave to get scattered and absorbed which in turn results in the degradation and attenuation of received optical signal. Besides the effects of the constituents, the refractive index at each point in the medium varies randomly in time due to the circulation of

---

Y.K. Baykal (✉)  
Çankaya University, Etimesgut, Ankara, Turkey  
e-mail: y.baykal@cankaya.edu.tr

air in the atmosphere and circulation of water in underwater medium. Random refractive index in time and space is simply known as the turbulence. Atmospheric turbulence is developed mainly by the fluctuations in the temperature, pressure and humidity but dominated by the temperature fluctuations. Turbulence in an underwater medium on the other hand is developed mainly by the fluctuations in the salinity and the temperature but dominated by the salinity fluctuations. The overall effect of turbulence on the received optical signal is an integrated one which is composed of the wavelength,  $\lambda$ , link length,  $L$ , the structure constant,  $C_n^2$  (a measure of how large the refractive index fluctuations are) in the atmosphere. The overall effect in the underwater medium is composed of the wavelength, link length, the rate of dissipation of kinetic energy per unit mass of fluid, the rate of dissipation of mean-squared temperature, the Kolmogorov inner scale, a parameter that defines the ratio of temperature to salinity contributions to the refractive index spectrum. The effect of turbulence on the optical beam depends on the strength of turbulence which changes the statistical behaviour of the medium which in turn changes the statistics of the random amplitude and phase fluctuations imposed by the random medium. The measure of turbulence strength in the atmosphere is given by the plane wave scintillation index known to be  $1.24C_n^2k^{7/6}L^{11/6}$  where  $k = 2\pi/\lambda$  is the wave number. Turbulent regime in the atmosphere is weak, moderate, strong and extremely strong when  $1.24C_n^2k^{7/6}L^{11/6}$  is  $\ll 1$ ,  $\sim 1$ ,  $> 1$  and  $\gg 1$ , respectively.

## 2.2 Degrading Effects of Turbulence

The random changes in the refractive index impose random variations in the amplitude and phase of the optical wave propagating in the turbulent medium. The randomly varying amplitude and phase in turn cause the degradation in the propagating optical wave which results in a degraded optical signal at the receiver of an optical wireless telecommunication or imaging system.

In the absence of turbulence, a finite-sized optical beam faces diffraction which broadens the beam as it propagates in the deterministic medium. Diffraction starts to be effective after a link distance of  $\alpha_s^2/\lambda$ ,  $\alpha_s$  being the size of the optical source at the transmitter plane. Diffraction angle is proportional to  $\lambda/\alpha_s$ . Broadening of the beam due to diffraction occurring in the absence of turbulence becomes larger when turbulence is present. Due to diffraction and refraction in turbulence, the instantaneous and the average intensity profile exhibit more beam spread at the receiver plane.

One other important degradation imposed by turbulence is the fluctuations in the intensity known as the scintillations which is quantified by the metric scintillation index. The scintillations impose signal dependent noise in the reception, thus degrade the performance quality of the optical wireless telecommunication system by reducing the bit error rate. The scintillations show different behaviour at the

receiver plane depending on the type of the optical source employed, wavelength, link length, strength of turbulence and the receiver coordinate.

When the coherent laser source beam wave propagates through turbulence, its coherence property is disturbed that makes the beam much less coherent, i.e. the beam becomes partially coherent or even incoherent at the receiver plane. In other words, coherence radius of the beam, which is defined as the radius of the area over which the optical field remains correlated, becomes smaller as the beam propagates in the turbulent medium. Smaller coherent patches make especially heterodyne and homodyne detection (coherent detection) difficult.

Another degradation of the optical beam wave due to turbulence arises because of the random fluctuations of the phase which cause the phase front of the optical wave become distorted. Especially in imaging systems, such phase fronts need to be corrected at the receiver through adaptive optics techniques. The phase fluctuations also become the reason for the angle of arrival fluctuations. Large angle of arrival fluctuations degrade the reception of the optical signal especially when the field of view of the receiver is narrow.

Turbulence also has effect on the effective radius of curvature of the optical beam that degrades the focusing of the beam on the required spot. Other parameters which are degraded by the presence of turbulence are the propagation factor, also known as the  $M^2$  factor, being regarded as a beam quality factor.

## 2.3 Power Spectra of Turbulence in Free Space Optics (FSO), Slant Satellite and Underwater Links

In the evaluation of turbulence effects, the random medium is modelled by eddies of various sizes in the continuum form. The eddies can be thought of as lenses. Thus, the random medium is composed of continuum of lenses starting from a minimum scale size known as the inner scale of turbulence to the maximum scale size known as the outer scale of turbulence. The scale size of the eddies being inversely proportional to the spatial frequency in the power spectrum of turbulence, the inner scale corresponds to the maximum spatial frequency and the outer scale corresponds to the minimum spatial frequency. The optical wave propagating in this continuum of lenses faces reflection, refraction, scattering, diffraction and interference which in turn results in the fluctuations of the amplitude and the phase of the optical wave. The effect of the eddies of all scale sizes are integrated in the power spectrum model of turbulence.

In the atmosphere, the most well-known power spectrum of turbulence is the Kolmogorov spectrum which is presented as [1]

$$\Phi_n(\kappa) = 0.033C_n^2\kappa^{-11/3}, \quad 1/L_0 \leq \kappa < 1/\ell_0 \quad (2.1)$$

where  $\kappa = 2\pi/\ell$  is the scalar spatial frequency,  $\ell$  being the scale of turbulence, i.e. the size of the turbulent eddy,  $\ell_0$  and  $L_0$  are the inner and outer scale of turbulence, respectively. Typical values of these scales in the atmosphere are  $\ell_0 = 1$  mm and  $L_0 = 25$  m but in the Kolmogorov presentation  $\ell_0 = 0$  and  $L_0 = \infty$  are taken. We note that the Kolmogorov spectrum in Eq. (2.1) is valid for horizontal wireless optical communication links where  $C_n^2$  is a constant. More general form of the turbulence power spectrum in which the inner scale, outer scale and the height variations of  $C_n^2$  are introduced is known as von Kármán spectrum given by [1]

$$\Phi_n(\kappa, \eta) = 0.033 C_n^2(\eta) \exp(\kappa^2/\kappa_m^2) / (\kappa^2 + \kappa_0^2)^{11/6}, \quad 0 \leq \kappa < \infty \quad (2.2)$$

where  $\eta$  is the propagation distance,  $\kappa_m = 5.92/\ell_0$  and  $\kappa_0 = 2\pi/L_0$ .

Kolmogorov presentation of the turbulence power spectrum does not exactly fit in some low altitude atmospheres [2], upper troposphere and stratosphere [3, 4]. In such media, it is more convenient to model the atmospheric turbulence with another power spectrum known as non-Kolmogorov which is given by [5]

$$\Phi_n(\kappa, \eta) = A(\alpha) \tilde{C}_n^2(\eta) \frac{\exp(\kappa^2/\kappa_m^2)}{(\kappa^2 + \kappa_0^2)^{\alpha/2}}, \quad 0 \leq \kappa < \infty, \quad 3 < \alpha < 4. \quad (2.3)$$

where  $\alpha$  is the power law exponent of non-Kolmogorov turbulence power spectrum,  $\eta$  denotes the fixed height of the horizontal link,  $c(\alpha) = [(2\pi/3) \Gamma(5 - 0.5\alpha) A(\alpha)]^{1/(\alpha-5)}$ ,  $\Gamma(\cdot)$  is the gamma function,  $A(\alpha) = 0.25\pi^{-2} \Gamma(\alpha - 1) \cos(0.5\pi\alpha)$ ,  $\kappa_m = c(\alpha)/\ell_0$ ,  $\tilde{C}_n^2(\eta)$  is the generalized structure constant in non-Kolmogorov turbulence having the unit of  $\text{m}^{3-\alpha}$ . In horizontal links, when  $\alpha = 11/3$ ,  $\tilde{C}_n^2(\eta)$  reduces to the structure constant  $C_n^2$  for Kolmogorov turbulence. Again for  $\alpha = 11/3$ , Eq. (2.3) correctly reduces to the von Kármán spectral density and additionally for  $\ell_0 = 0$  and  $L_0 = \infty$  reduces to the Kolmogorov spectral density.

In non-Kolmogorov turbulence, the equivalence of the structure constant for non-Kolmogorov turbulence in horizontal links is formulated as [6]

$$\tilde{C}_n^2 = \frac{N(\alpha)}{D(\alpha)} C_n^2 \quad (2.4)$$

where  $N(\alpha) = 0.5\Gamma(\alpha)(2\pi)^{-11/6+\alpha/2}(\lambda L)^{11/6-\alpha/2}$ ,  $D(\alpha) = -\Gamma(1 - \frac{\alpha}{2}) [\Gamma(\frac{\alpha}{2})]^2 \Gamma(\alpha - 1) \cos(\frac{\alpha\pi}{2}) \sin(\frac{\pi\alpha}{4})$ .

Note that negative sign in  $D(\alpha)$  is missing in [6]. In satellite links,  $C_n^2$  varies depending on the height from the ground. This variation is expressed by several models, the best known being the Hufnagel–Valley model [1] which is expressed for the slant paths in general as

$$C_n^2(h) = 0.00594 \left(\frac{w}{27}\right)^2 (10^{-5}h)^{10} \exp\left(-\frac{h}{1000}\right) + 2.7 \times 10^{-16} \exp\left(-\frac{h}{1500}\right) + A \exp\left(-\frac{h}{100}\right) \quad (2.5)$$

where  $h$  is the height from the ground expressed in meters,  $A$  is the nominal value of  $C_n^2(h=0)$  in  $\text{m}^{-2/3}$ ,  $w$  is the rms wind speed in m/s whose height dependence can be found from Eq. (12.2) of [1]. Here  $h = \eta \cos \varsigma$ ,  $\varsigma$  is the zenith angle. Inserting  $h = \eta \cos \varsigma$  into Eq. (2.5)

$$C_n^2(\eta) = 0.00594(w/27)^2 (10^{-5}\eta \cos \varsigma)^{10} \exp(-\eta \cos \varsigma/1000) + 2.7 \times 10^{-16} \exp(-\eta \cos \varsigma/1500) + A \exp(-\eta \cos \varsigma/100) \quad (2.6)$$

which is valid for flat Earth model. Introducing the equivalence of the structure constant provided by Eq. (2.4) for the slant satellite links, we obtain

$$C_n^2(\alpha, \eta) = \frac{N(\alpha)}{D(\alpha)} C_n^2(\eta). \quad (2.7)$$

The last power spectrum presented in this section cover the random underwater medium which is given by [7]

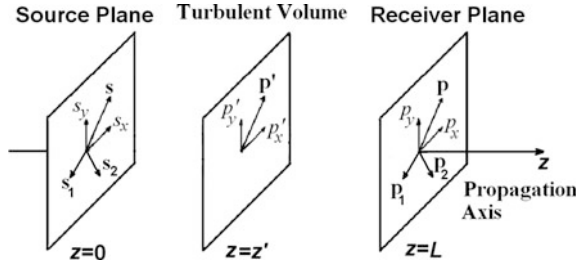
$$\Phi_n(\kappa) = 0.388 \times 10^{-8} \varepsilon^{-1/3} \kappa^{-11/3} \left[ 1 + 2.35(\kappa \ell)^{2/3} \right] \frac{X_T}{w^2} \times (w^2 e^{-A_T \delta} + e^{-A_S \delta} - 2w e^{-A_{TS} \delta}) \quad (2.8)$$

where the eddy thermal diffusivity and the diffusion of salt are assumed to be equal,  $A_T = 1.863 \times 10^{-2}$ ,  $A_S = 1.9 \times 10^{-4}$ ,  $A_{TS} = 9.41 \times 10^{-3}$ ,  $\delta = 8.284 (\kappa \eta)^{4/3} + 12.978 (\kappa \eta)^2$ ,  $\varepsilon$  is the rate of dissipation of kinetic energy per unit mass of fluid,  $X_T$  is the rate of dissipation of mean-squared temperature,  $\ell$  is the Kolmogorov inner scale,  $w$  is a unitless parameter that defines the ratio of temperature to salinity contributions to the refractive index spectrum. In oceanic water,  $w$  changes from  $-5$  to  $0$  where it attains  $-5$  when temperature-induced turbulence dominates and  $0$  when salinity-induced optical turbulence dominates.

## 2.4 Rytov Method

A geometrical sketch illustrating the propagation geometry and definitions of the parameters employed in the formulations of this and the following sections is shown in Fig. 2.1.

**Fig. 2.1** Propagation geometry



The incident field at the laser exit plane ( $z = 0$ ) is  $u^{\text{inc}}(\mathbf{s}, z = 0)$  where  $\mathbf{s} = (s_x, s_y)$  is the transverse source coordinate and  $z$  is the propagation axis. The free space field  $u^{\text{FS}}(\mathbf{p}, z)$  at the receiver point  $\mathbf{r} = (\mathbf{p}, z) = (p_x, p_y, z)$  in the absence of turbulence can be found by using the Huygens–Fresnel principle as [1]

$$u^{\text{FS}}(\mathbf{p}, z) = \frac{k \exp(ikz)}{2\pi iz} \int_{-\infty}^{\infty} \int_{-\infty}^{\infty} d^2\mathbf{s} u^{\text{inc}}(\mathbf{s}, z = 0) \exp\left[\frac{ik}{2z}(\mathbf{s} - \mathbf{p})^2\right]. \quad (2.9)$$

In the presence of turbulence, by using the free space field,  $u^{\text{FS}}(\mathbf{p}, z)$  given by Eq. (2.9), the field at the receiver plane is found by Rytov method as [8, 9]

$$u(\mathbf{p}, z) = u^{\text{FS}}(\mathbf{p}, z) \exp[\psi(\mathbf{p}, z)]. \quad (2.10)$$

Here

$$\begin{aligned} \psi(\mathbf{p}, z) &= \chi(\mathbf{p}, z) + iS(\mathbf{p}, z) = \frac{k^2}{2\pi u^{\text{FS}}(\mathbf{p}, z)} \int_{V'} d^3\mathbf{r}' n_1(\mathbf{p}', z') u^{\text{FS}}(\mathbf{p}', z') \\ &\times \frac{\exp(ik|\mathbf{r} - \mathbf{r}'|)}{|\mathbf{r} - \mathbf{r}'|}, \end{aligned} \quad (2.11)$$

is the fluctuations of the complex amplitude in turbulence,  $V'$  is the scattering volume,  $\chi(\mathbf{p}, z)$  and  $S(\mathbf{p}, z)$  are the log-amplitude and phase fluctuations in turbulence, respectively,  $\mathbf{r}' = (\mathbf{p}', z') = (p'_x, p'_y, z')$ ,  $d^3\mathbf{r}' = dp'_x dp'_y dz'$ ,  $\frac{\exp(ik|\mathbf{r} - \mathbf{r}'|)}{|\mathbf{r} - \mathbf{r}'|}$  term presents the Green's function,  $n_1$  is the random part of the refractive index which is [10]

$$n_1(p'_x, p'_y, z') = \int_{-\infty}^{\infty} \int_{-\infty}^{\infty} \exp(i\kappa_x p'_x + i\kappa_y p'_y) dZ_n(\kappa_x, \kappa_y, z') \quad (2.12)$$

where the integrations are implicit with respect to  $\kappa_x, \kappa_y$  which are the spatial frequencies in  $x$  and  $y$  directions,  $dZ_n(\kappa_x, \kappa_y, z')$  is the random amplitude of the

spectrum of the refractive index fluctuations. Using [8–10] since for the major portions of the beam,  $(p_x - p'_x)$  and  $(p_y - p'_y)$  are much smaller than  $(z - z')$ , the Green's function in Eq. (2.11) is approximated as

$$\frac{\exp(ik|\mathbf{r} - \mathbf{r}'|)}{|\mathbf{r} - \mathbf{r}'|} \approx \exp \left\{ ik \left[ (z - z') + \frac{(p_x - p'_x)^2 + (p_y - p'_y)^2}{2(z - z')} \right] \right\} / (z - z') \quad (2.13)$$

Employing Eqs. (2.12) and (2.13) in Eq. (2.11), the complex amplitude fluctuations at the receiver,  $z = L$  is

$$\psi(\mathbf{p}, L) = \int_0^L dz' \int_{-\infty}^{\infty} \int_{-\infty}^{\infty} H(p_x, p_y, L, \kappa_x, \kappa_y, z') dZ_n(\kappa_x, \kappa_y, z') \quad (2.14)$$

where

$$\begin{aligned} H(.) &= k^2 / [2\pi(L - z') u^{\text{FS}}(\mathbf{p}, z)] \int_{-\infty}^{\infty} \int_{-\infty}^{\infty} dp_x dp_y \exp(i\kappa_x p'_x + i\kappa_y p'_y) \\ &\times u^{\text{FS}}(\mathbf{p}', z') \exp \left\{ ik \left[ (z - z') + \frac{(p_x - p'_x)^2 + (p_y - p'_y)^2}{2(z - z')} \right] \right\} / (z - z'). \end{aligned} \quad (2.15)$$

Using Eq. (2.14) together with Eq. (2.15) and making use of  $\psi(\mathbf{p}, L) = \chi(\mathbf{p}, L) + iS(\mathbf{p}, L)$  from Eq. (2.11), the log-amplitude fluctuations term is found to be [8–10]

$$\begin{aligned} \chi(\mathbf{p}, L) &= 0.5[\psi(\mathbf{p}, L) + \psi^*(\mathbf{p}, L)] = \int_0^L dz' \int_{-\infty}^{\infty} \int_{-\infty}^{\infty} T_1(p_x, p_y, L, \kappa_x, \kappa_y, z') \\ &\times dZ_n(\kappa_x, \kappa_y, z') \end{aligned} \quad (2.16)$$

where  $dZ_n^*(\kappa_x, \kappa_y, z') = dZ_n(-\kappa_x, -\kappa_y, z')$  and

$$\begin{aligned} T_1(p_x, p_y, L, \kappa_x, \kappa_y, z') &= 0.5[H(p_x, p_y, L, \kappa_x, \kappa_y, z') \\ &+ H^*(p_x, p_y, L, -\kappa_x, -\kappa_y, z')] \end{aligned} \quad (2.17)$$

Again, using Eq. (2.14) together with Eq. (2.15) and making use of  $\psi(\mathbf{p}, L) = \chi(\mathbf{p}, L) + iS(\mathbf{p}, L)$  from Eq. (2.11), the phase fluctuations term is found to be

$$S(\mathbf{p}, L) = 0.5i[\psi^*(\mathbf{p}, L) - \psi(\mathbf{p}, L)] = \int_0^L dz' \int_{-\infty}^{\infty} \int_{-\infty}^{\infty} T_2(p_x, p_y, L, \kappa_x, \kappa_y, z') \times dZ_n(\kappa_x, \kappa_y, z') \quad (2.18)$$

where

$$T_2(p_x, p_y, L, \kappa_x, \kappa_y, z') = 0.5i[H^*(p_x, p_y, L, -\kappa_x, -\kappa_y, z') - H(p_x, p_y, L, \kappa_x, \kappa_y, z')] \quad (2.19)$$

Thus, the Rytov method solution of the field at the receiver plane in an unguided medium is found by using Eq. (2.14) in Eq. (2.10). Furthermore, the correlation functions of the log-amplitude and the phase fluctuations are obtained by employing Eqs. (2.16) and (2.18). The details of the derivation of the correlation functions can be found in [9].

## 2.5 Extended Huygens–Fresnel Principle

In the absence of turbulence, the field at the receiver plane is given by the Huygens–Fresnel principle as [1]

$$u(\mathbf{p}, L) = \frac{\exp(ikL)}{\lambda iL} \int_{-\infty}^{\infty} \int_{-\infty}^{\infty} d^2\mathbf{s} u^{\text{inc}}(\mathbf{s}, z=0) \exp\left(\frac{ik}{2L}|\mathbf{s} - \mathbf{p}|^2\right). \quad (2.20)$$

Basically, with the Huygens–Fresnel principle, one can find the field at the receiver of an optical wireless communication system by applying a spatial convolution integral to the spatial incident field and the spatial spherical wave response medium. When the medium of interest is a random one due to the presence of turbulence, then the field at the receiver of an optical wireless communication system is obtained by applying the spatial convolution integral to the spatial incident field and the spatial spherical wave response of the random medium which is presented as

$$u(\mathbf{p}, L) = \frac{\exp(ikL)}{\lambda iL} \int_{-\infty}^{\infty} \int_{-\infty}^{\infty} d^2\mathbf{s} u^{\text{inc}}(\mathbf{s}, z=0) \exp\left(\frac{ik}{2L}|\mathbf{s} - \mathbf{p}|^2\right) \exp[i\psi(\mathbf{s}, \mathbf{p})] \quad (2.21)$$



where  $\psi(\mathbf{s}, \mathbf{p})$  is the solution to Rytov method given by Eq. (2.11) that presents the random part of the complex phase of a spherical wave propagating from the source point  $(\mathbf{s}, z = 0)$  to the receiver point  $(\mathbf{p}, L)$ . By using Eq. (2.21), many important entities used in unguided optical communication system, such as the average received intensity, intensity fluctuations in the received optical signal, field correlations, intensity correlations and bit error rate (BER) can be formulated.

## 2.6 Average Received Intensity

Using Eq. (2.21), for a coherent source, the instantaneous received intensity at the receiver plane  $I(\mathbf{p}, L) = u(\mathbf{p}, L)u^*(\mathbf{p}, L)$  is found to be [1]

$$\begin{aligned} I(\mathbf{p}, L) &= \frac{1}{(\lambda L)^2} \int_{-\infty}^{\infty} \int_{-\infty}^{\infty} \mathbf{d}^2 \mathbf{s}_1 \int_{-\infty}^{\infty} \int_{-\infty}^{\infty} \mathbf{d}^2 \mathbf{s}_2 u^{\text{inc}}(\mathbf{s}_1, z = 0) u^{\text{inc}} * (\mathbf{s}_2, z = 0) \\ &\quad \times \exp\left(\frac{ik}{2L} |\mathbf{s}_1 - \mathbf{p}|^2\right) \exp\left(-\frac{ik}{2L} |\mathbf{s}_2 - \mathbf{p}|^2\right) \\ &\quad \times \exp[\psi(\mathbf{s}_1, \mathbf{p})] \exp[\psi^*(\mathbf{s}_2, \mathbf{p})], \end{aligned} \quad (2.22)$$

and the average received intensity  $\langle I(\mathbf{p}, L) \rangle = \langle u(\mathbf{p}, L)u^*(\mathbf{p}, L) \rangle$  is obtained as

$$\begin{aligned} \langle I(\mathbf{p}, L) \rangle &= \frac{1}{(\lambda L)^2} \int_{-\infty}^{\infty} \int_{-\infty}^{\infty} \mathbf{d}^2 \mathbf{s}_1 \int_{-\infty}^{\infty} \int_{-\infty}^{\infty} \mathbf{d}^2 \mathbf{s}_2 u^{\text{inc}}(\mathbf{s}_1, z = 0) u^{\text{inc}} * (\mathbf{s}_2, z = 0) \\ &\quad \times \exp\left(\frac{ik}{2L} |\mathbf{s}_1 - \mathbf{p}|^2\right) \exp\left(-\frac{ik}{2L} |\mathbf{s}_2 - \mathbf{p}|^2\right) \\ &\quad \times \langle \exp[\psi(\mathbf{s}_1, \mathbf{p})] \exp[\psi^*(\mathbf{s}_2, \mathbf{p})] \rangle. \end{aligned} \quad (2.23)$$

where  $\langle \exp[\psi(\mathbf{s}_1, \mathbf{p})] \exp[\psi^*(\mathbf{s}_2, \mathbf{p})] \rangle = \exp\left[-\frac{1}{2} D_\psi(\mathbf{s}_1, \mathbf{s}_2)\right]$ ,  $D_\psi(\mathbf{s}_1, \mathbf{s}_2)$  being the wave structure function.

## 2.7 Intensity and Power Scintillation Index

The scintillations in turbulence can be calculated using both the Rytov method and the extended Huygens–Fresnel principle. In the first part of this section, Rytov method solution for the scintillation index will be presented which will be followed

by the extended Huygens–Fresnel principle solution. In the Rytov solution, first the log-amplitude correlation function must be found since the scintillation index is 4 times the log-amplitude correlation function [11].

The correlation function of the log-amplitude fluctuations at the receiver plane ( $z = L$ ) is defined by

$$B_\chi(\mathbf{p}_1, \mathbf{p}_2, L) = \langle \chi(\mathbf{p}_1, L) \chi(\mathbf{p}_2, L) \rangle \quad (2.24)$$

Inserting the log-amplitude fluctuations given by Eq. (2.16) in Eq. (2.24) [9]

$$\begin{aligned} B_\chi(\mathbf{p}_1, \mathbf{p}_2, L) = & 2\pi \int_0^L dz' \int_{-\infty}^{\infty} d\kappa_x \int_{-\infty}^{\infty} d\kappa_y T_1(p_{x_1}, p_{y_1}, L, \kappa_x, \kappa_y, z') \\ & \times T_1(p_{x_2}, p_{y_2}, L, -\kappa_x, -\kappa_y, z') \Phi_n(\kappa) \end{aligned} \quad (2.25)$$

where  $\Phi_n(\kappa)$  is the power spectrum of turbulence,  $\kappa = (\kappa_x^2 + \kappa_y^2)^{1/2}$ ,  $T_1(\cdot)$  is provided by Eq. (2.17) [10]. Derivation of Eq. (2.25) can be found in Appendix A of [9]. At the receiver point  $\mathbf{p}$ , the scintillation index by Rytov method is  $m^2 = 4B_\chi(\mathbf{p}, \mathbf{p}, L)$  [8] where  $B_\chi(\mathbf{p}, \mathbf{p}, L)$  is the correlation function of the log-amplitude fluctuations given by Eq. (2.25) which is evaluated at  $\mathbf{p}_1 = \mathbf{p}_2 = \mathbf{p}$ .

In the evaluation by using the extended Huygens–Fresnel principle, the scintillation index is defined as

$$m^2 = \langle I^2(\mathbf{p}, L) \rangle / \langle I(\mathbf{p}, L) \rangle^2 - 1 \quad (2.26)$$

where  $\langle I(\mathbf{p}, L) \rangle$  is given in Eq. (2.23). To find  $\langle I^2(\mathbf{p}, L) \rangle$ , we start with Eq. (2.22) and obtain

$$\begin{aligned} \langle I^2(\mathbf{p}, L) \rangle = & \frac{1}{(\lambda L)^4} \int_{-\infty}^{\infty} \int_{-\infty}^{\infty} d^2\mathbf{s}_1 \int_{-\infty}^{\infty} \int_{-\infty}^{\infty} d^2\mathbf{s}_2 \int_{-\infty}^{\infty} \int_{-\infty}^{\infty} d^2\mathbf{s}_3 \int_{-\infty}^{\infty} \int_{-\infty}^{\infty} d^2\mathbf{s}_4 u^{\text{inc}}(\mathbf{s}_1) u^{\text{inc}*}(\mathbf{s}_2) \\ & \times u^{\text{inc}}(\mathbf{s}_3) u^{\text{inc}*}(\mathbf{s}_4) \exp\left(\frac{ik}{2L} |\mathbf{s}_1 - \mathbf{p}|^2\right) \exp\left(-\frac{ik}{2L} |\mathbf{s}_2 - \mathbf{p}|^2\right) \\ & \times \exp\left(\frac{ik}{2L} |\mathbf{s}_3 - \mathbf{p}|^2\right) \exp\left(-\frac{ik}{2L} |\mathbf{s}_4 - \mathbf{p}|^2\right) \Gamma_4^m(\mathbf{s}_1, \mathbf{s}_2, \mathbf{s}_3, \mathbf{s}_4, \mathbf{p}), \end{aligned} \quad (2.27)$$

where  $\Gamma_4^m(\cdot) = \langle \exp[\psi(\mathbf{s}_1, \mathbf{p})] \exp[\psi^*(\mathbf{s}_2, \mathbf{p})] \exp[\psi(\mathbf{s}_3, \mathbf{p})] \exp[\psi^*(\mathbf{s}_4, \mathbf{p})] \rangle$  is the fourth order coherence function of the medium. Evaluating Eq. (2.26) at the receiver origin, i.e. at  $\mathbf{p} = (p_x, p_y) = (0, 0)$  [12, 13].

$$\begin{aligned} \Gamma_4^m(\cdot) = & [1 + 2B_\chi(\mathbf{s}_1 - \mathbf{s}_3) + 2B_\chi(\mathbf{s}_2 - \mathbf{s}_4)] \exp[-0.5D_\psi(\mathbf{s}_1 - \mathbf{s}_2) \\ & - 0.5D_\psi(\mathbf{s}_3 - \mathbf{s}_4) - 0.5D_\psi(\mathbf{s}_2 - \mathbf{s}_3) - 0.5D_\psi(\mathbf{s}_1 - \mathbf{s}_4) \\ & + 0.5D_\psi(\mathbf{s}_1 - \mathbf{s}_3) + 0.5D_\psi(\mathbf{s}_2 - \mathbf{s}_4) + iD_{\chi S}(\mathbf{s}_2 - \mathbf{s}_4) - iD_{\chi S}(\mathbf{s}_1 - \mathbf{s}_3)], \end{aligned} \quad (2.28)$$

where  $D_\psi(\mathbf{s}_r - \mathbf{s}_q) = \frac{2|\mathbf{s}_r - \mathbf{s}_q|^2}{\rho_0^2}$  with  $\mathbf{r} = 1, 2, 3$  and  $\mathbf{q} = 2, 3, 4$  is the wave structure function,  $D_{\chi S}(\mathbf{s}_r - \mathbf{s}_q) = |\mathbf{s}_r - \mathbf{s}_q|^2 / \rho_{\chi S}^2$  is the log-amplitude phase structure function,  $B_\chi(\mathbf{s}_m - \mathbf{s}_n) = \sigma_\chi^2 \exp(-|\mathbf{s}_m - \mathbf{s}_n|^2 / \rho_0^2)$  is the log-amplitude correlation function,  $\rho_0 = (0.545 C_n^2 k^2 L)^{-3/5}$  is the coherence length of a spherical wave propagating in the turbulent medium,  $\sigma_\chi^2 = 0.124 C_n^2 k^{7/6} L^{11/6}$  is the variance of log amplitude for spherical waves, and  $\rho_{\chi S} = (0.114 k^{13/6} C_n^2 L^{5/6})^{-1/2}$  is the coherence length of log-amplitude and phase. Using Kolmogorov spectrum with zero inner scale in Eq. (2.28), the condition of validity of the wave structure function is  $|\mathbf{s}_r - \mathbf{s}_q| \ll (\lambda L)^{1/2}$  [12]. In Eq. (2.28), Gaussian statistics for the log amplitude and phase fluctuations and  $B_\chi < 1$  is employed to expand  $\exp[2B_\chi(\mathbf{s}_1 - \mathbf{s}_3) + 2B_\chi(\mathbf{s}_2 - \mathbf{s}_4)]$  as  $[1 + 2B_\chi(\mathbf{s}_1 - \mathbf{s}_3) + 2B_\chi(\mathbf{s}_2 - \mathbf{s}_4)]$ . For this reason, the scintillation index to be obtained will be valid in weak atmospheric turbulence.

In the receiver aperture averaging evaluations, the power scintillation index is required in which the effect of the finite receiver aperture is included in the scintillation formulation. For this purpose, the average power detected by a finite-sized receiver having Gaussian aperture function is found from

$$\langle P \rangle = \int_{-\infty}^{\infty} \int_{-\infty}^{\infty} \langle I(\mathbf{p}) \rangle \exp\left(-\frac{|\mathbf{p}|^2}{R^2}\right) d^2 \mathbf{p} \quad (2.29)$$

where Gaussian aperture function is assumed,  $R$  is the radius of the receiver aperture size and  $\langle I(\mathbf{p}) \rangle$  is given by Eq. (2.23). The average of the square of the power as detected by a finite-sized aperture receiver having a Gaussian aperture function is found as [12]

$$\langle P^2 \rangle = \int_{-\infty}^{\infty} \int_{-\infty}^{\infty} \int_{-\infty}^{\infty} \int_{-\infty}^{\infty} \langle I(\mathbf{p}_1) I(\mathbf{p}_2) \rangle \exp\left(-\frac{|\mathbf{p}_1|^2 + |\mathbf{p}_2|^2}{R^2}\right) d^2 \mathbf{p}_1 d^2 \mathbf{p}_2 \quad (2.30)$$

where using Eq. (2.22)

$$\begin{aligned}
\langle I(\mathbf{p}_1)I(\mathbf{p}_2) \rangle &= \frac{1}{(\lambda L)^4} \int_{-\infty}^{\infty} \int_{-\infty}^{\infty} d^2\mathbf{s}_1 \int_{-\infty}^{\infty} \int_{-\infty}^{\infty} d^2\mathbf{s}_2 \int_{-\infty}^{\infty} \int_{-\infty}^{\infty} d^2\mathbf{s}_3 \int_{-\infty}^{\infty} \int_{-\infty}^{\infty} d^2\mathbf{s}_4 u^{\text{inc}}(\mathbf{s}_1) u^{\text{inc}*}(\mathbf{s}_2) \\
&\quad \times u^{\text{inc}}(\mathbf{s}_3) u^{\text{inc}*}(\mathbf{s}_4) \exp \left[ \frac{jk}{2L} \left( |\mathbf{p}_1 - \mathbf{s}_1|^2 - |\mathbf{p}_1 - \mathbf{s}_2|^2 + |\mathbf{p}_2 - \mathbf{s}_3|^2 - |\mathbf{p}_2 - \mathbf{s}_4|^2 \right) \right] \\
&\quad \times \langle \exp[\psi(\mathbf{s}_1, \mathbf{p}_1) + \psi^*(\mathbf{s}_2, \mathbf{p}_1) + \psi(\mathbf{s}_3, \mathbf{p}_2) + \psi^*(\mathbf{s}_4, \mathbf{p}_2)] \rangle.
\end{aligned} \tag{2.31}$$

The fourth-order medium coherence function given in the last line of Eq. (2.31) is used as given in [12, 13]. The power scintillation is defined as [14]

$$m_p^2 = \frac{\langle (P - \langle P \rangle)^2 \rangle}{\langle P \rangle^2} = \frac{\langle P^2 \rangle}{\langle P \rangle^2} - 1 \tag{2.32}$$

from which the receiver aperture averaging factor is defined as [14]

$$G_R = m_p^2 / m_p^2 \Big|_{R=0} = m^2 \tag{2.33}$$

where  $m_p^2 \Big|_{R=0} = m^2$  is the scintillation index for a point aperture given by Eq. (2.26).

## 2.8 Bit Error Rate

The formula for the average bit error rate  $\langle \text{BER} \rangle$  in turbulence as a function of the average signal to noise ratio  $\langle \text{SNR} \rangle$  is given by [15] for a receiver detecting on-off keying (OOK) modulation as

$$\langle \text{BER} \rangle = \frac{1}{2} \int_0^{\infty} p_I(s) \text{erfc} \left( \frac{\langle \text{SNR} \rangle s}{2\sqrt{2} \langle i_s \rangle} \right) ds \tag{2.34}$$

where  $\text{erfc}(\cdot)$  is the complementary error function,  $\langle i_s \rangle$  is the detector signal current,  $s$  is the integration variate and  $p_I(s)$  is the probability density function of the intensity. Below, the general formulation of  $\langle \text{BER} \rangle$  in strong turbulence is provided which is known to yield also the weak turbulence results [15]. In strong turbulence, the intensity can be statistically defined by the gamma-gamma distribution whose probability density function is given by [16]

$$p_I(s) = \frac{2(\alpha\beta)^{(\alpha+\beta)/2}}{\Gamma(\alpha)\Gamma(\beta)} \left( \frac{s}{\langle i_s \rangle} \right)^{(\alpha+\beta)/2-1} K_{\alpha-\beta} \left( 2\sqrt{\frac{\alpha\beta s}{\langle i_s \rangle}} \right), \quad s > 0, \tag{2.35}$$

where  $K$  is the modified Bessel function of the second kind,  $\Gamma(\cdot)$  is the gamma function,  $\alpha = \frac{1}{\exp(m_{LS}^2)-1}$  and  $\beta = \frac{1}{\exp(m_{SS}^2)-1}$ . The  $m_{LS}^2$  and  $m_{SS}^2$  are the large-scale and small-scale scintillation indices, respectively [1, 17] whose derivations can be obtained by using  $m^2 = 4B_\chi(\mathbf{p}, \mathbf{p}, L)$  where the log-amplitude correlation function  $B_\chi(\mathbf{p}, \mathbf{p}, L)$  is obtained from Eq. (2.25) by replacing the power spectrum of turbulence  $\Phi_{n,e}(\kappa)$  by the effective spectral density of the index of refraction fluctuations given below,

$$\Phi_{n,e}(\kappa) = 0.033C_n^2\kappa^{-11/3} \left[ \exp\left(-\frac{\kappa^2}{\kappa_x^2}\right) + \frac{\kappa^{11/3}}{(\kappa^2 + \kappa_y^2)^{11/6}} \right]. \quad (2.36)$$

The effective spectral density introduces [1, 17] the amplitude spatial filtering described by the large-scale,  $\kappa_x$  and the small-scale,  $\kappa_y$  spatial frequency cutoffs. In Eq. (2.36), the inner and outer scales of turbulences are taken to be zero and infinity. The details of the derivations of  $m_{LS}^2$  and  $m_{SS}^2$  can be found in [18]. It is known that <BER> found by using the gamma–gamma distribution is a close fit not only in strong turbulence but also in weak and moderate fluctuation regions as well [1]. To be complete, the probability density function of the intensity valid in weak turbulence which has a log-normal distribution is given below [19]

$$p_I(u) = \frac{1}{m\sqrt{2\pi}u} \exp\left\{-\frac{[\ln(u) + \frac{1}{2}m^2]^2}{2m^2}\right\}, \quad u > 0 \quad (2.37)$$

where  $m^2$  is the on-axis scintillation index.

## 2.9 Beam Effects in Turbulent Medium

The average intensity, scintillation index and thus the <BER> of an optical wave at the receiver of an unguided optical communication system, after passing through turbulent medium, exhibit wide variations depending on the type of incidence (source) used. The basic formulations of the average intensity, scintillation index, and <BER> are shown in the above sections. In this section, the average intensity and the scintillation index formulations will be revised by introducing a general type optical beam as the incidence [20, 21].

At the laser exit plane ( $z = 0$ ), the incident field for the  $(n,m)$ th single-mode off-axis Hermite–Gaussian beam is given by [20]

$$u_{\ell nm}^{\text{inc}}(s_x, s_y, z = 0) = A_{\ell nm} \exp(-i\theta_{\ell nm}) H_n(a_{x\ell n}s_x + b_{x\ell n}) H_m(a_{y\ell m}s_y + b_{y\ell m}) \\ \times \exp\left[-\frac{k}{2}(\alpha_{x\ell n}s_x^2 + \alpha_{y\ell m}s_y^2)\right] \exp[-i(V_{x\ell n}s_x + V_{y\ell m}s_y)], \quad (2.38)$$

where  $\alpha_{x\ell n} = \frac{1}{kx_{\ell n}^2} + \frac{i}{F_{x\ell n}}$ ,  $\alpha_{y\ell m} = \frac{1}{ky_{\ell m}^2} + \frac{i}{F_{y\ell m}}$ ,  $k$  is the wave number,  $\mathbf{s} = (s_x, s_y)$  is the transverse source coordinate,  $z$  is the propagation axis, index  $\ell nm$  presents the mode,  $\ell$  being the number of the set of the multimode content,  $nm$  is the specific mode within the  $\ell$ th set,  $A_{\ell nm}$  is the amplitude of the field of the mode ( $\ell nm$ ) at the origin of the source plane, i.e. at  $(s_x = s_y = z = 0)$ ,  $\theta_{\ell nm}$  is the constant phase factor.  $H_n$  and  $H_m$  are Hermite polynomials of order  $n$  and  $m$  that specify the field distributions in the  $s_x, s_y$  directions,  $a_{x\ell n}$  and  $a_{y\ell m}$  are the complex parameters determining the width of the Hermite polynomials in the  $s_x, s_y$  directions,  $b_{x\ell n}$  and  $b_{y\ell m}$  are the complex parameters characterizing the displacement of the Hermite polynomials in the  $s_x, s_y$  directions,  $\alpha_{x\ell n}$  and  $F_{x\ell n}$  are the source size of the Gaussian beam and the focal length in  $s_x$  direction and similarly  $\alpha_{y\ell m}$  and  $F_{y\ell m}$  present the source size of the Gaussian beam and the focal length in  $s_y$  direction,  $i = (-1)^{1/2}$ ,  $V_{x\ell n} = V_{xr\ell n} + iV_{xi\ell n}$  and  $V_{y\ell m} = V_{yr\ell m} + iV_{yi\ell m}$  are the complex displacement parameters,  $V_{xr\ell n}$ ,  $V_{xi\ell n}$  denote the real and imaginary components of  $V_{x\ell n}$  and  $V_{yr\ell m}$ ,  $V_{yi\ell m}$  denote the real and imaginary components of  $V_{y\ell m}$ . Defining the general type beam as the superposition of the sets of the off-axis Hermite–Gaussian beams in Eq. (2.38), the incident field at the laser exit plane ( $z = 0$ ) for the general type beam is

$$u^{\text{inc}}(s_x, s_y, z = 0) = \sum_{\ell=1}^N \sum_{(n,m)} u_{\ell nm}^{\text{inc}}(s_x, s_y, z = 0) \quad (2.39)$$

$\sum_{(n,m)}$  shows the summation of the single-mode incident fields within the  $\ell$ th set of multimode contents,  $\sum_{\ell=1}^N$  denotes the summation over the different sets of multimode contents which indicates that there are  $N$  different sets of multimode contents. Inserting Eq. (2.38) into Eq. (2.39), the incident field of the general type beam becomes

$$u^{\text{inc}}() = \sum_{\ell=1}^N \sum_{(n,m)} A_{\ell nm} \exp(-i\theta_{\ell nm}) H_n(a_{x\ell n}s_x + b_{x\ell n}) H_m(a_{y\ell m}s_y + b_{y\ell m}) \\ \times \exp\left[-\frac{k}{2}(\alpha_{x\ell n}s_x^2 + \alpha_{y\ell m}s_y^2)\right] \exp[-i(V_{x\ell n}s_x + V_{y\ell m}s_y)], \quad (2.40)$$

which presents a very wide class of beams such as the spherical, plane, Gaussian, higher order single-mode, multimode, off-axis Hermite–Gaussian, Hermite–

sinusoidal-Gaussian, higher order annular, flat-topped-Gaussian. The parameter definitions of all these beams can be found in [20] and in Table 1 of [21].

Inserting Eq. (2.40) into Eq. (2.23), the average intensity  $\langle I(\mathbf{p}, L) \rangle = \langle u(\mathbf{p}, L) u^*(\mathbf{p}, L) \rangle$  of a general type optical beam in turbulence is

$$\begin{aligned}
 \langle I(\mathbf{p}, L) \rangle = & \frac{1}{(\lambda L)^2} \int_{-\infty}^{\infty} \int_{-\infty}^{\infty} \mathbf{d}^2 \mathbf{s}_1 \int_{-\infty}^{\infty} \int_{-\infty}^{\infty} \mathbf{d}^2 \mathbf{s}_2 \sum_{\ell=1}^N \sum_{(n,m)} A_{\ell nm} e^{-i\theta_{\ell nm}} H_n(a_{x\ell n} s_x + b_{x\ell n}) \\
 & \times H_m(a_{y\ell m} s_y + b_{y\ell m}) \exp \left[ -\frac{k}{2} (\alpha_{x\ell n} s_x^2 + \alpha_{y\ell m} s_y^2) \right] \exp [-i(V_{x\ell n} s_x + V_{y\ell m} s_y)] \\
 & \times \sum_{\ell=1}^N \sum_{(n,m)} A_{\ell nm}^* \exp(i\theta_{\ell nm}) H_n^*(a_{x\ell n} s_x + b_{x\ell n}) H_m^*(a_{y\ell m} s_y + b_{y\ell m}) \\
 & \times \exp \left[ -\frac{k}{2} (\alpha_{x\ell n}^* s_x^2 + \alpha_{y\ell m}^* s_y^2) \right] \exp [i(V_{x\ell n}^* s_x + V_{y\ell m}^* s_y)] \\
 & \times \exp \left( \frac{ik}{2L} |\mathbf{s}_1 - \mathbf{p}|^2 \right) \exp \left( -\frac{ik}{2L} |\mathbf{s}_2 - \mathbf{p}|^2 \right) \langle \exp[\psi(\mathbf{s}_1, \mathbf{p})] \exp[\psi^*(\mathbf{s}_2, \mathbf{p})] \rangle.
 \end{aligned} \tag{2.41}$$

For atmospheric turbulence, under the quadratic approximation for the Rytov's phase structure function  $\langle \exp[\psi(\mathbf{s}_1, \mathbf{p}) + \psi^*(\mathbf{s}_2, \mathbf{p})] \rangle \cong \exp[-\rho_0^{-2}(\mathbf{s}_1 - \mathbf{s}_2)^2]$ ,  $\rho_0 = (0.545 C_n^2 k^2 L)^{-3/5}$  is the coherence length of a spherical wave propagating in the turbulent medium. Equation (2.41) is evaluated for the general beam, which yields in the limiting cases the average intensity in turbulence for various beam types such as the flat-topped, annular, cos-Gaussian, sine-Gaussian, cosh-Gaussian, sinh-Gaussian and their higher order counterparts [21].

To introduce the beam effects in the formulation of the scintillation index by Rytov method, we start with  $m^2 = 4B_\chi(\mathbf{p}, \mathbf{p}, L)$  [6] where  $B_\chi(\mathbf{p}, \mathbf{p}, L)$  in Eq. (2.25) is evaluated by introducing the general beam type incident field in Eq. (2.40). Thus,  $T_1(p_x, p_y, L, \kappa_x, \kappa_y, z')$  in Eq. (2.17),  $H(p_x, p_y, L, \kappa_x, \kappa_y, z')$  in Eq. (2.15) and in turn  $u^{\text{FS}}(\mathbf{p}, z)$  in Eq. (2.9) are evaluated by the use of  $u^{\text{inc}}(s_x, s_y, z=0)$  given by Eq. (2.40). With this procedure, for the general type beam, using Eq. (2.40) in Eq. (2.9), it is found that [20]

$$\begin{aligned}
 u^{\text{FS}}(\mathbf{p}, z) = & \sum_{\ell=1}^N \sum_{(n,m)} \frac{k \exp(ikz) A_{\ell nm} \exp(-i\theta_{\ell nm})}{2\pi i z} \int_{-\infty}^{\infty} \int_{-\infty}^{\infty} \mathbf{d}^2 \mathbf{s} H_n(a_{x\ell n} s_x + b_{x\ell n}) \\
 & \times H_m(a_{y\ell m} s_y + b_{y\ell m}) \exp \left[ -\frac{k}{2} (\alpha_{x\ell n} s_x^2 + \alpha_{y\ell m} s_y^2) \right] \\
 & \times \exp [-i(V_{x\ell n} s_x + V_{y\ell m} s_y)] \exp \left[ \frac{ik}{2z} (\mathbf{s} - \mathbf{p})^2 \right].
 \end{aligned} \tag{2.42}$$

Performing the integration over  $\mathbf{s} = (s_x, s_y)$  by using Eq. (7.374.8) of [22], and after some algebraic rearrangements,  $u^{\text{FS}}(\mathbf{p}, z)$  becomes

$$u^{\text{FS}}(\mathbf{p}, z) = \sum_{\ell=1}^N \sum_{(n,m)} A_{\ell nm} e^{ikz} e^{-i\theta_{\ell nm}} f_n(p_x) f_m(p_y) \quad (2.43)$$

where

$$f_n(p_x) = \left[ 1 - \frac{2ia_{x\ell n}^2 z}{k(1 + i\alpha_{x\ell n} z)} \right]^{n/2} \frac{1}{(1 + i\alpha_{x\ell n} z)^{1/2}} \exp \left[ -\frac{iV_{x\ell n}^2 z}{2k(1 + i\alpha_{x\ell n} z)} \right] \\ \times \exp \left[ -\frac{k\alpha_{x\ell n}}{2(1 + i\alpha_{x\ell n} z)} p_x^2 \right] \exp \left[ -\frac{iV_{x\ell n}}{(1 + i\alpha_{x\ell n} z)} p_x \right] H_n(\beta_{1x\ell n} + \beta_{2x\ell n} p_x),$$

$\beta_{2x\ell n} = a_{x\ell n}(1 + i\alpha_{x\ell n} z)^{-1/2} \left[ 1 - iz \left( \frac{2a_{x\ell n}^2}{k} - \alpha_{x\ell n} \right) \right]^{-1/2}$ ,  $\beta_{1x\ell n} = \beta_{2x\ell n} \left[ \frac{a_{x\ell n} V_{x\ell n} z + kb_{x\ell n}(1 + i\alpha_{x\ell n} z)}{ka_{x\ell n}} \right]$  and  $f_m(p_y)$  is found by replacing  $x$  and  $n$  by  $y$  and  $m$ , respectively in  $f_n(p_x)$ . Inserting Eq. (2.43) into Eq. (2.15), inserting the thus found  $H(p_x, p_y, L, \kappa_x, \kappa_y, z')$  in Eq. (2.17),  $T_1(p_x, p_y, L, \kappa_x, \kappa_y, z')$  for the general type beam is obtained. Through the use of this  $T_1(p_x, p_y, L, \kappa_x, \kappa_y, z')$  in Eq. (2.25), the log-amplitude correlation function for the general beam type is found as [20]

$$B_\chi(\mathbf{p}_1, \mathbf{p}_2, L) = \pi \text{Re} \left\{ \int_0^L d\eta \int_0^\infty \kappa d\kappa \int_0^{2\pi} d\theta [M_1(\mathbf{p}_1, \mathbf{p}_2, \eta, \kappa, \theta) \right. \\ \left. + M_2(\mathbf{p}_1, \mathbf{p}_2, \eta, \kappa, \theta)] \Phi_n(\kappa) \right\}, \quad (2.44)$$

where  $\mathbf{\kappa} = \kappa e^{i\theta} \Rightarrow \kappa_x = \kappa \cos \theta, \kappa_y = \kappa \sin \theta, \kappa = |\mathbf{\kappa}| = (\kappa_x^2 + \kappa_y^2)^{1/2} \Rightarrow d^2 \mathbf{\kappa} = d\kappa_x d\kappa_y = \kappa d\kappa d\theta$ ,

$$M_1(\mathbf{p}_1, \mathbf{p}_2, L, \eta, \kappa, \theta) = N(\mathbf{p}_1, L, \eta, \kappa, \theta) N(\mathbf{p}_2, L, \eta, -\kappa, \theta) / [D(\mathbf{p}_1, L) D(\mathbf{p}_2, L)] \\ M_2(\mathbf{p}_1, \mathbf{p}_2, L, \eta, \kappa, \theta) = N(\mathbf{p}_1, L, \eta, \kappa, \theta) N^*(\mathbf{p}_2, L, \eta, \kappa, \theta) / [D(\mathbf{p}_1, L) D^*(\mathbf{p}_2, L)]$$

$N(\cdot)$ ,  $D(\mathbf{p}, L)$  and other relevant parameters in Eq. (2.44) are defined in [20].

Then, the scintillation index for the general type beams is found by  $m^2 = 4B_\chi(\mathbf{p}, \mathbf{p}, L)$  where  $B_\chi(\mathbf{p}, \mathbf{p}, L)$  is provided by Eq. (2.44).

The scintillation index in atmospheric optical communication links for many optical incidences such as flat-topped-Gaussian [23], laser arrays [24], higher order cos-Gaussian, cosh-Gaussian [25] are examined which are reviewed in [26]. Beam type effects on the scintillations are also examined lately in underwater medium for optical plane and spherical waves [27] and multimode laser beams [28].



Beam effects on the scintillations can also be examined by utilizing the extended Huygens–Fresnel principle. For this purpose, we start with Eq. (2.26), employ Eq. (2.41) and use Eq. (2.27) after inserting the  $u^{\text{inc}}(s_x, s_y, z = 0)$  from Eq. (2.40). Through this approach, in atmospheric turbulence, we have lately investigated the effects of beam types on the scintillation index for different excitations such as the annular, flat-topped [13], off-axis Gaussian [29] and cos-Gaussian, cosh Gaussian [30].

The effects of beam types on the  $\langle \text{BER} \rangle$  in atmospheric turbulence can be formulated by inserting Eq. (2.44) in  $m^2 = 4B_\chi(\mathbf{p}, \mathbf{p}, L)$ . This scintillation index formula is then employed in Eqs. (2.35) or (2.37) which in turn is inserted in Eq. (2.34). Through this approach, we have reported the  $\langle \text{BER} \rangle$  for various incidences such as the annular, flat-topped [15, 31] and sinusoidal-Gaussian [32].

## 2.10 Mitigation Methods to Reduce Turbulence Effects

The degradation of the received optical signal can be mitigated by using several techniques. As also pointed out in the above sections, the degradation of the signal can occur in the form of the received intensity profile, fluctuations in the intensity known as scintillations and  $\langle \text{BER} \rangle$  that effect the overall performance of optical wireless communication systems operating in the atmosphere or in underwater medium. Such degradations manifest themselves in the form of further beam spread due to turbulence and signal dependent multiplicative noise.

Numerous works appear in the literature that studies the mitigation methods to reduce turbulence effects. Basics of some of the important applications in the mitigation of turbulence, such as the use of nondiffracting beams, scintillation reduction techniques involving the use of various beam types, receiver aperture averaging, partially coherent sources, error control coding and phase conjugation are mentioned to a certain extent below. The elaboration of these techniques can be traced in the indicated references.

The average intensity profiles in turbulence are scrutinized under various sources [21]. Some excitations happen to confine the beam more at the receiver plane. Especially, nondiffracting optical beams such as Bessel beams operating in a turbulent medium seem to be advantages in this sense [33]. However, working range of the link operating with Bessel beams is too short in this case.

Reduction in the scintillation noise is obtained through various techniques. It is well known for a long time that an optical plane wave scintillates 2.5 times more than the optical spherical wave and the Gaussian beam wave exhibits some interim scintillation values [1, 8, 11], i.e. the shape of the intensity of the incident optical beam has a considerable role in shaping the fluctuations of the intensity at the receiver of an unguided optical communication system. This fact is lately investigated in detail for many different optical source beam intensities. Some of these are mentioned in the above section where the beam type effects are summarized in [26].

These studies reveal that under the same medium conditions, i.e. under the same wavelength, link length, inner scale, outer scale and the structure constant for the atmosphere, and under the same wavelength, rate of dissipation of kinetic energy per unit mass of fluid, rate of dissipation of mean-squared temperature, Kolmogorov inner scale, temperature and salinity contributions to the refractive index spectrum for the ocean, when the optical source intensity profile is varied, some source configurations become advantageous in reducing the scintillations.

Another technique to reduce the effects of turbulence is to employ large aperture receivers in optical wireless communication links. Finite receiver aperture has a smoothing effect on the received power fluctuations known as aperture averaging which is studied in the past [12, 34–38] and lately for various optical incidences [39–41].

Use of partially coherent optical beams also yield smaller scintillations as compared to coherent laser beams. Partial coherence effects on the scintillations are studied in detail [13, 42–47]. However, the discrepancy in the use of partially coherent sources is the decrease in the data rates that can be transmitted in the unguided optical communication systems. This is due to the fact that coherent laser beams can be modulated at much higher data rates as compared to the modulation rates of partially coherent or incoherent sources.

In some atmospheric optics applications, use of error control coding is used to mitigate turbulence-induced fading [48, 49]. Use of some codes such as the Reed–Solomon or Bose, Chaudhuri, and Hocquenghem or Hamming is known to improve the performance of atmospheric optics links especially at high signal to noise ratios as compared to cases where no coding is used.

Finally, we just mention that one other mitigation method employed in atmospheric optics systems is the use of phase conjugation techniques in adaptive optics [50] in which the aberrations formed in the wavefront after passing through turbulence are corrected.

## 2.11 Sample Results

In this section, some sample results of the above given formulations are referenced in order to better discuss the main findings of turbulence impact. These are the results of the evaluations of Eqs. (2.4), (2.32), (2.33) and (2.34) which are found in [6, 15, 40, 41], respectively. The other detailed results can also be traced from these references. We state these results as that the equivalent structure constant in non-Kolmogorov turbulence versus Kolmogorov structure constant have constant slopes at different power laws, when the hollow core of the annular beam becomes wider, power scintillation increases, the receiver aperture averaging is more effective at the larger flatness parameter with increasing receiver aperture sizes and thinner annular beams show smaller average BER in strong turbulence.

## 2.12 Conclusions and Future Directions

In wireless optical communication systems, the medium plays a crucial role in determining the performance characteristics. Especially, when the refractive index of the medium varies in a random nature as in turbulence, it becomes even more difficult to stay within the predetermined performance criteria. The amplitude and the phase of the received signal become distorted in a random manner, as the result, different techniques are to be applied to overcome the adverse effects of turbulence.

In this chapter, we have reviewed the nature of turbulence in atmospheric and underwater medium. The effect of turbulence on the wireless optical communication systems operating in the atmosphere and in underwater are investigated. The basics of the formulations employed to obtain the average intensity, the scintillation index and BER are presented. The mitigation methods, such as aperture averaging, optical beam type used and partial coherence, to reduce the degrading effects of turbulence are reported.

Even though the nature of turbulence in terms of its spectrum presentations are known to a big extent, still further work, especially experimental data is needed to better describe the atmospheric and underwater turbulence in specific media. Again, the basic formulations, such as the Rytov and extended Huygens–Fresnel principle are widely employed to obtain the system parameters. However, further simulation methods to be presented in future will ease to better understand and apply the results in practical optical communication systems. Many different approaches such as the use of multi-input multi output configurations, optical heterodyne reception techniques and employment of different optical sources, understanding anisotropic turbulence, height variations of turbulence in underwater medium, ultraviolet communication systems and marine environment defined as the water atmosphere interface, are some important topics foreseen to be further scrutinized in future in this area.

## References

1. Andrews, L.C., Philips, R.L.: *Laser beam propagation through random media*. SPIE, Bellingham, Washington (2005)
2. Tunick, A.: Analysis of free-space laser signal intensity over a 2.33 km optical path. *Proc. SPIE* **6708**, 670802 (2007)
3. Kyrakis, D.T., Wissler, J., Keating, D.D.B., Preble, A.J., Bishop, K.P.: Measurement of optical turbulence in the upper troposphere and lower stratosphere. *Proc. SPIE* **2120**, 43–55 (1994)
4. Stribling, B.E., Welsh, B.M., Roggemann, M.C.: Optical propagation in non-Kolmogorov atmospheric turbulence. *Proc. SPIE* **2471**, 181–196 (1995)
5. Toselli, I., Andrews, L.C., Phillips, R.L., Ferrero, V.: Free-space optical system performance for laser beam propagation through non-Kolmogorov turbulence. *Opt. Eng.* **47**, 026003 (2008)
6. Baykal, Y., Gerçekcioğlu, H.: Equivalence of structure constants in non-Kolmogorov and Kolmogorov spectra. *Opt. Lett.* **36**, 4554–4556 (2011)

7. Nikishov, V.V., Nikishov, V.I.: Spectrum of turbulent fluctuations of the sea-water refraction index. *Int. J. Fluid Mech. Res.* **27**, 82–98 (2000)
8. Tatarskii, V.I.: Wave propagation in a turbulent medium. McGraw-Hill, New York (1961)
9. Baykal, Y.: Correlation and structure functions of Hermite-sinusoidal-Gaussian laser beams in a turbulent atmosphere. *J. Opt. Soc. Am. A* **21**, 1290–1299 (2004)
10. Ishimaru, A.: Fluctuations in the parameters of spherical waves propagating in a turbulent atmosphere. *Radio Sci.* **4**, 295–305 (1969)
11. Ishimaru, A.: Wave propagation and scattering in random media. Academic Press, San Diego (1978)
12. Wang, S.J., Baykal, Y., Plonus, M.A.: Receiver-aperture averaging effects for the intensity fluctuation of a beam wave in the turbulent atmosphere. *J. Opt. Soc. Am.* **73**, 831–837 (1983)
13. Baykal, Y., Eyyuboğlu, H.T., Cai, Y.: Scintillations of partially coherent multiple Gaussian beams in turbulence. *Appl. Opt.* **48**, 1943–1954 (2009)
14. Andrews, L.C., Phillips, R.L., Hopen, C.Y.: Laser beam scintillation with applications. SPIE, Bellingham (2001)
15. Tyson, R.K.: Bit-error rate for free-space adaptive optics laser communications. *J. Opt. Soc. Am. A* **19**, 753–758 (2002)
16. Gerçekcioğlu, H., Baykal, Y.: BER of annular and flat-topped beams in strong turbulence. *Opt. Commun.* **298–299**, 18–21 (2013)
17. Andrews, L.C., Phillips, R.L., Hopen, C.Y., Al-Habash, M.A.: Theory of optical scintillation. *J. Opt. Soc. Am. A* **16**, 1417–1429 (1999)
18. Gerçekcioğlu, H., Baykal, Y.: Scintillation index of flat-topped Gaussian laser beam in strongly turbulent medium. *J. Opt. Soc. Am. A* **28**, 1540–1544 (2011)
19. Tyson, R.K., Canning, D.E.: Indirect measurement of a laser communications bit error rate reduction with low order adaptive optics. *Appl. Opt.* **42**, 4239 (2003)
20. Baykal, Y.: Formulation of correlations for general-type beams in atmospheric turbulence. *J. Opt. Soc. Am. A* **23**, 889–893 (2006)
21. Arpali, Ç., Yazıcıoğlu, C., Eyyuboğlu, H.T., Arpali, S.A., Baykal, Y.: Simulator for general-type beam propagation in turbulent atmosphere. *Opt. Express* **14**, 8918–8928 (2006)
22. Gradshteyn, I.S., Ryzhik, I.M.: Tables of Integrals, Series and Products. Academic Press, New York (2000)
23. Baykal, Y., Eyyuboğlu, H.T.: Scintillation index of flat-topped-Gaussian beams. *Appl. Opt.* **45**, 3793–3797 (2006)
24. Eyyuboğlu, H.T., Baykal, Y., Cai, Y.: Scintillations of laser array beams. *Appl. Phys. B* **92**, 265–271 (2008)
25. Arpali, S.A., Eyyuboğlu, H.T., Baykal, Y.: Scintillation index of higher order cos-Gaussian, cosh-Gaussian and annular beams. *J. Mod. Opt.* **55**, 227–239 (2008)
26. Baykal, Y., Eyyuboğlu, H.T., Cai, Y.: Effect of beam types on the scintillations: a review. *Proc. SPIE* **7200**, 720002 (2009)
27. Ata, Y., Baykal, Y.: Scintillations of optical plane and spherical waves in underwater turbulence. *J. Opt. Soc. Am. A* **31**, 1552–1556 (2014)
28. Baykal, Y.: Intensity fluctuations of multimode laser beams in underwater medium. *J. Opt. Soc. Am. A* **32**, 593–598 (2015)
29. Baykal, Y., Eyyuboğlu, H.T., Cai, Y.: Partially coherent off-axis Gaussian beam scintillations. *J. Mod. Opt.* **57**, 1221–1227 (2010)
30. Baykal, Y., Eyyuboğlu, H.T., Çil, C.Z., Cai, Y., Korotkova, O.: Intensity fluctuations of partially coherent cos Gaussian and cosh Gaussian beams in atmospheric turbulence. *J. Opt.* **13**, 055709 (2011)
31. Gerçekcioğlu, H., Baykal, Y.: BER of annular and flat-topped beams in non-Kolmogorov weak turbulence. *Opt. Commun.* **286**, 30–33 (2013)
32. Gerçekcioğlu, H., Baykal, Y.: Scintillation and BER for optimum sinusoidal Gaussian beams in weak non-Kolmogorov turbulence. *Opt. Commun.* **320**, 1–5 (2014)
33. Lukin, I.P.: Mean intensity of a fundamental Bessel beam in turbulent atmosphere. *Opt. Eng.* **53**, 096104 (2014)

34. Fried, D.L.: Aperture averaging of scintillation. *J. Opt. Soc. Am.* **57**, 169–175 (1967)
35. Kon, A.I.: Averaging of spherical-wave fluctuations over a receiving aperture. *Radiophys. Quantum Electron.* **12**, 122–124 (1969)
36. Lutomirski, R.F., Yura, H.T.: Aperture-averaging factor of a fluctuating light signal. *J. Opt. Soc. Am.* **59**, 1247–1248 (1969)
37. Churnside, J.H.: Aperture averaging of optical scintillations in the turbulent atmosphere. *Appl. Opt.* **30**, 1982–1994 (1991)
38. Andrews, L.C.: Aperture-averaging factor for optical scintillations of plane and spherical waves in the atmosphere. *J. Opt. Soc. Am. A* **9**, 597–600 (1992)
39. Andrews, L.C., Phillips, R.L., Hopen, C.Y.: Aperture averaging of optical scintillations: power fluctuations and the temporal spectrum. *Waves Random Media* **10**, 53–70 (2000)
40. Kamacıoğlu, C., Baykal, Y., Yazgan, E.: Averaging of receiver aperture for flat-topped incidence. *Opt. Laser Technol.* **52**, 91–95 (2013)
41. Kamacıoğlu, C., Baykal, Y., Yazgan, E.: Receiver aperture averaging of annular beams propagating through turbulent atmosphere. *Opt. Eng.* **52**, 126103 (2013)
42. Kon, A.I., Tatarskii, V.I.: On the theory of the propagation of partially coherent light beams in a turbulent atmosphere. *Radiophys. Quantum Electron.* **15**, 1187–1192 (1972)
43. Belenkii, M.S., Mironov, V.L.: Turbulent distortions of the spatial coherence of a laser beam. *Sov. J. Quantum Electron.* **7**, 287–290 (1977)
44. Leader, J.C.: Intensity fluctuations resulting from a spatially partially coherent light propagating through atmospheric turbulence. *J. Opt. Soc. Am.* **69**, 73–84 (1979)
45. Banakh, V.A., Buldakov, V.M., Mironov, V.L.: Intensity fluctuations of a partially coherent light beam in a turbulent atmosphere. *Opt. Spektrosk.* **54**, 1054–1059 (1983)
46. Baykal, Y., Plonus, M.A., Wang, S.J.: The scintillations for weak atmospheric turbulence using a partially coherent source. *Radio Sci.* **18**, 551–556 (1983)
47. Korotkova, O., Andrews, L.C., Phillips, R.L.: A model for a partially coherent Gaussian beam in atmospheric turbulence with application in lasercom. *Opt. Eng.* **43**, 330–341 (2004)
48. Zhu, X., Kahn, J.M.: Performance bounds for coded free-space optical communications through atmospheric turbulence channels. *IEEE Trans. Commun.* **51**, 1233–1239 (2003)
49. Uysal, M., Li, J., Meng, Y.: Error rate performance analysis of coded free-space optical links over gamma-gamma atmospheric turbulence channels. *IEEE Trans. Wireless Commun.* **5**, 1229–1233 (2006)
50. Tyson, R.K.: *Principles of Adaptive Optics*. CRC Press, Taylor & Francis Group, Florida (2011)

Optical Wireless Communications

An Emerging Technology

Uysal, M.; Capsoni, C.; Ghassemlooy, Z.; Boucouvalas, A.; Udvary, E. (Eds.)

2016, XX, 634 p. 290 illus., 188 illus. in color.,

Hardcover

ISBN: 978-3-319-30200-3